Drug Development and Industrial Pharmacy, 2010; 36(11): 1377–1387

informa
healthcare

ORIGINAL ARTICLE

Application of rotatable central composite design in the preparation and optimization of poly(lactic-*co*-glycolic acid) nanoparticles for controlled delivery of paclitaxel

Sivacharan Kollipara, Girish Bende, Snehalatha Movva and Ranendra Saha

Formulation Development & Pharmacokinetics Laboratory, Pharmacy Group, Birla Institute of Technology & Science, Pilani, Rajasthan, India

Abstract

Context: Polymeric carrier systems of paclitaxel (PCT) offer advantages over only available formulation Taxol® in terms of enhancing therapeutic efficacy and eliminating adverse effects. *Objective*: The objective of the present study was to prepare poly (lactic-*co*-glycolic acid) nanoparticles containing PCT using emulsion solvent evaporation technique. *Methods*: Critical factors involved in the processing method were identified and optimized by scientific, efficient rotatable central composite design aiming at low mean particle size and high entrapment efficiency. Twenty different experiments were designed and each formulation was evaluated for mean particle size and entrapment efficiency. The optimized formulation was evaluated for in vitro drug release, and absorption characteristics were studied using in situ rat intestinal permeability study. *Results*: Amount of polymer and duration of ultrasonication were found to have significant effect on mean particle size and entrapment efficiency. First-order interactions of amount of miglyol with amount of polymer were significant in case of mean particle size, whereas second-order interactions of polymer were significant in mean particle size and entrapment efficiency. The developed quadratic model showed high correlation ($R^2 > 0.85$) between predicted response and studied factors. The optimized formulation had low mean particle size (231.68 nm) and high entrapment efficiency (95.18%) with 4.88% drug content. The optimized formulation showed controlled release of PCT for more than 72 hours. In situ absorption study showed faster and enhanced extent of absorption of PCT from nanoparticles compared to pure drug. *Conclusion*: The poly (lactic-*co*-glycolic acid) nanoparticles containing PCT may be of clinical importance in enhancing its oral bioavailability.

Key words: *Central composite design; optimization; paclitaxel; PLGA nanoparticles; response surface methodology*

Introduction

Paclitaxel (PCT) is one of the major breakthroughs in cancer research[1]. PCT binds to β-subunit of tubulin and hyper-stabilizes microtubule structure[2,3]. This leads to the disruption of normal dynamics of microtubules and consequently causes cell death. Another mechanism is also proposed in which PCT induces apoptosis in cancer cells by binding to B-cell leukemia protein 2, an apoptosis-stopping protein, and arrests its function[4]. Because of its unique mechanisms, PCT is found to be effective against various types of cancers such as breast, ovarian, lung, head and neck cancers, Kaposi's sarcoma, small cell lung cancer, malignant gliomas, and brain metastases[5–10]. PCT, chemically known as (1*S*, 2*S*, 3*R*,4*S*,7*R*,9*S*,10*S*,12*R*,15*S*)-4,12-diacetoxy-15-{[(2*R*,3*S*)-3-(benzoylamino)-2-hydroxy-3-phenylpropanoyl]oxy}-1,9- dihydroxy-10, 14, 17, 17-tetramethyl-11-oxo-6-oxatetracyclo [11.3.1.0~3,10~.0~4,7~] heptadec-13-en-2-yl benzoate), is a high-molecular-weight drug (M_w, 845 Da) with high hydrophobicity (log *P*, 3.96) and poor aqueous solubility (<0.03 mg/L)[11]. Because of its limited solubility and dissolution and its affinity for metabolizing enzymes (CYP3A4) and p-glycoprotein, the oral

Address for correspondence: Ranendra Saha, Dean, Faculty Division-III, Birla Institute of Technology & Science, Pilani, Rajasthan, India. Tel: +91 1596 515284 Ext. 284 / 267, Fax: + 91-1596-244183. E-mail: rnsaha@bits-pilani.ac.in

(Received 5 Sep 2009; accepted 16 Apr 2010)

ISSN 0363-9045 print/ISSN 1520-5762 online © Informa UK, Ltd.
DOI: 10.3109/03639045.2010.487263

bioavailability of PCT is found to be less than 10%[12–15]. Moreover, PCT has very low therapeutic index and at therapeutic concentrations it shows several adverse effects[15]. These limitations led to the development of nonaqueous solution (Taxol®, Bristol-Myers Squibb, New York, USA) of PCT (6 mg/mL) dissolved in 1:1 (%, v/v) mixture consisting of Cremophor EL (polyoxyethylated castor oil) and dehydrated alcohol for intravenous administration. This formulation is to be diluted with suitable parenteral fluid before intravenous infusion. However, there are major complications associated with the use of this formulation such as development of hypersensitivity reactions, nephrotoxicity, neurotoxicity, vasodilation, lethargy, and hypotension due to the presence of Cremophor EL[16–18]. Over the past few years, efforts were made in developing delivery systems for PCT that were devoid of Cremophor EL[19]. Abraxane® is one of the successful outcomes, in which PCT is bound to albumin and indicated for the treatment of breast cancer after failure of combination chemotherapy[20]. However, alternative dosage forms have also been investigated including liposomes[21], microparticles[22,23], parenteral emulsions[24,25], nanoparticles[26,27], self-emulsifying drug delivery systems[28], and mixed micelles[29]. Among novel drug delivery systems, nanoparticles have been considered as potential and effective carrier for delivery of anticancer agents. Encapsulation of drugs in nanoparticles was found to alter the tissue distribution and pharmacokinetics leading to enhancement in therapeutic efficacy and reduction of side effects[30]. Additionally, nanoparticles were found to accumulate in the leaky solid tumor by a mechanism named enhanced permeation and retention leading to enhanced efficacy and safety[31]. Moreover, it has also been demonstrated that anticancer drugs encapsulated in nanoparticles can bypass the resistance mediated by P-glycoprotein resulting in enhanced drug concentration at the target site[32].

Preformed polymers such as poly (lactic-*co*-glycolic acid) (PLGA) have generated wide interest in nanoparticle research because of their ease of use, biocompatibility, and biodegradability. Out of numerous procedures available for preparation of PLGA nanoparticles, emulsion solvent evaporation is a classical and well-established procedure[33]. This method consists of emulsification of water-immiscible organic solvent containing polymer and drug in aqueous surfactant solution under high-energy agitation. Removal of organic solvent by vacuum or heat leads to the formation of nanoparticles. Sometimes an oil such as miglyol can be added in organic phase as a reservoir for drug after evaporation of organic solvent. In this method, several factors impact the formation of nanoparticles with acceptable size, polydispersity, and good entrapment efficiency, such as amount of polymer, duration and intensity of agitation, amount of oil in organic phase, surfactant concentration in aqueous phase, and pH of aqueous phase. It is very difficult to assess the impact of these factors individually or in combination indicating the necessity of mathematical modeling in establishing the quantitative relationship between these factors. Application of design of experimentation (DOE) technique can be successfully implemented for identification of explanatory variables that have significant effect on response properties[34,35]. Complex designs such as central composite design (CCD) can be applied for the optimization[36,37]. CCD consists of embedded factorial design, group of star points for the estimation of curvature, and center points for the determination of experimental reproducibility.

In the present study, PCT-containing polymeric nanoparticles providing controlled drug delivery were prepared using emulsion solvent evaporation technique. The rotatable central composite design (RCCD) was used to investigate and optimize the impact of critical factors such as amount of miglyol, amount of polymer, and duration of agitation on the response properties such as mean particle size and entrapment efficiency. In addition, the optimized formulation was assessed for in vitro drug release and in situ rat intestinal absorption.

Experimental

Materials

PCT (assay 99.95%) was generously gifted by Dr. Reddy's Laboratories, Hyderabad, India. PLGA copolymer and Miglyol 810 were gifted by Purac, Nebraska, USA, and Sasol Chemicals, Hamburg, Germany, respectively. Polyvinyl alcohol was purchased from Sigma-Aldrich Chemicals Ltd., Miamisburg, USA. Analytical grade potassium dihydrogen phosphate, disodium hydrogen phosphate, sodium chloride, potassium chloride, and calcium chloride were purchased from S.D. Fine Chemicals Ltd., Mumbai, India. HPLC grade acetonitrile and dichloromethane were purchased from Spectrochem, Mumbai, India. Ultra pure water was prepared using a Milli-Q® water purification system (Millipore Co., Billerica, USA) and filtered (0.22 μm) before use. All other chemicals used in the study were of analytical grade.

Animals

Healthy young male Wistar rats with average weight 250 ± 25 g (12–15 weeks) were obtained from Central Animal Facility, BITS, Pilani, India. Animals were housed in groups of three in standard plastic cages and maintained at controlled conditions. Animals were acclimatized to study environment for 3 days prior to experimentation and a standard laboratory pellet food was provided with free access to water. The study protocol (IAEC/

RES/05/05–06a) was approved by Institutional Animal Ethics Committee (IAEC), BITS, Pilani. All the experimental procedures including disposal of carcass and euthanasia were in agreement with the guidelines set by IAEC, BITS, Pilani.

Chromatographic conditions

A Jasco HPLC system (Kyoto, Japan), consisting of PU-1580 pumps, AS-1559 auto–injector, and UV-1575 UV–visible detector, was used for analysis of the test samples. Mobile phase consisting of acetonitrile and 20 mM potassium dihydrogen phosphate (45:55, v/v) was degassed under vacuum and delivered in isocratic mode at a flow rate of 1 mL/min. The chromatographic separation was achieved on Lichrocart® RP_{18} reversed phase column (120 × 4.6 mm, 5 µm, Merck, New Jersey, USA). Following 50 µL injection of a sample, the column eluents were monitored at 230 nm for 10 minutes. The analysis was performed at ambient temperature after baseline stabilization for at least 30 minutes. Chromatographic data were acquired and processed using Borwin® (Jasco, Japan) software.

Preparation of nanoparticles

PLGA nanoparticles containing PCT were prepared by emulsion solvent evaporation technique. Briefly, the organic phase was prepared by dissolving accurate content of PLGA, miglyol, and drug (10 mg) in 1 mL of methylene chloride. Under moderate stirring conditions, the prepared organic phase was added into aqueous phase containing polyvinyl alcohol (2%, w/v) as a stabilizer. Immediately, the system was subjected to ultrasonication at energy output of 15 W in cycles of 30 seconds over a specified period of time. The resulting oil/water emulsion was stirred at room temperature for 12 hours for complete evaporation of methylene chloride. Obtained nanoparticles were centrifuged at 14,000 rpm at 25°C for 30 minutes (Remi Compufuge, Mumbai, India) and the surface-adsorbed drug was washed with phosphate-buffered saline. Finally, the prepared nanoparticles were freeze dried over a period of 12 hours (Maxi Dry Lyo, Heto, Germany) to obtain a free flowing powder.

Experimental design

A RCCD was implemented for the optimization of various response properties. Initially, preliminary studies were conducted to determine the critical factors involved in nanoparticles preparation using emulsion solvent evaporation technique. Based on preliminary studies, three critical factors namely amount of oil in the organic phase, amount of polymer, and duration of ultrasonication (at 15 W) were selected for the optimization of mean particle size and entrapment efficiency. Upper and lower limits for the individual factors, with which stable nanoparticles can be prepared, were identified in the preliminary studies. During the optimization trials, these values for critical factors were varied between the extreme levels as indicated in Table 1. In the present design, 20 different experiments were carried out to determine the model coefficients. The three factors implemented in the present study are summarized in Table 2. The design had a total of $2^k + 2k + n$ individual experiments, where k is the number of factors ($k = 3$) and n the number of experiments carried out at center points ($n = 6$) to evaluate experimental reproducibility. The first set involved 2^k experiments forming the main factorial design and second set involved $2k$ experiments, which were carried out at the star points, a distance ($\pm\alpha(2^{k/4})$) away from the center. The above CCD model was rotatable with $\alpha = \pm 1.68$. In total, 20 experiments were carried out randomly to avoid experimental bias.

Table 1. Identified critical factors and their levels investigated in central composite design.

	Transformed levels				
Critical factors	−1.68	−1	0	+1	+1.68
X_1 – Amount of miglyol (µL)	03.20	10.00	20.00	30.00	36.80
X_2 – Amount of PLGA (mg)	04.00	12.50	25.00	37.50	46.00
X_3 – Duration of sonication at 15 W (minutes)	01.28	04.00	08.00	12.00	14.72

Characterization of nanoparticles

The prepared nanoparticles were characterized for mean particle size and entrapment efficiency. In addition, the optimized formulation was also characterized for polydispersity index, drug content, and in vitro drug release.

Mean particle size and polydispersity

The mean particle size and polydispersity index of various batches were determined by photon correlation spectroscopy (PCS) technique using a particle size analyzer (3000HS-Zetasizer, Malvern Instruments Inc., Malvern, UK) equipped with He–Ne laser beam at a wavelength of 633 nm and 90° scattering angle. For each measurement, 2 mg of formulation was dispersed in 10 mL of previously sonicated and filtered Milli-Q® water. Obtained homogenous dispersion was immediately used for the determination of mean particle diameter and polydispersity index. The data acquisition and processing was performed using PCS software (Malvern Instruments Inc.).

Table 2. Rotatable central composite design for three factors at five different levels: X_1 = amount of miglyol, X_2 = amount of polymer, X_3 = duration of ultrasonication at 15 W.

Experiment no.	Order of experiment	Coded levels X_1	X_2	X_3	Experiment type	Experimental response: Mean particle size (nm)	Entrapment efficiency (%)
01	11	1.00	1.00	1.00	2^3 factorial design	315.40	84.85
02	15	1.00	1.00	−1.00		388.40	87.41
03	06	1.00	−1.00	1.00		237.10	97.83
04	03	1.00	−1.00	−1.00		271.60	88.71
05	10	−1.00	1.00	1.00		311.60	88.31
06	09	−1.00	1.00	−1.00		313.90	80.75
07	19	−1.00	−1.00	1.00		268.60	97.69
08	01	−1.00	−1.00	−1.00		324.70	84.25
09	18	0.00	1.68	0.00	Star design	344.60	73.37
10	02	0.00	−1.68	0.00		262.50	94.99
11	14	0.00	0.00	1.68		191.90	98.41
12	08	0.00	0.00	−1.68		306.00	89.98
13	05	1.68	0.00	0.00		254.10	85.77
14	13	−1.68	0.00	0.00		275.40	92.13
15	04	0.00	0.00	0.00	Center points (n = 6)	249.00	89.19
16	20	0.00	0.00	0.00		273.40	91.13
17	07	0.00	0.00	0.00		244.90	93.81
18	16	0.00	0.00	0.00		233.70	93.69
19	12	0.00	0.00	0.00		240.60	95.60
20	17	0.00	0.00	0.00		255.80	90.57
Coefficient of variation (%CV) at center points (n = 6)						5.56	2.61

Entrapment efficiency and drug content

For the determination of entrapment efficiency, 10 mg of lyophilized nanoparticles were digested in 2 mL of acetonitrile. The formed solution was centrifuged at 14,000 rpm for 10 minutes and the supernatant was suitably diluted with mobile phase and analyzed. The entrapment efficiency and drug content were calculated by using Equations (1) and (2):

$$\text{Entrapment efficiency} = \frac{\text{Amount of drug recovered in nanoparticles}}{\text{Total amount of drug added}} \times 100, \quad (1)$$

$$\text{Drug content} = \frac{\text{Amount of drug in nanoparticles}}{\text{Total amount of nanoparticles recovered}} \times 100. \quad (2)$$

Response surface modeling

An efficient technique of response surface methodology (RSM) for determining the influence of multiple factors was used for the response analysis and modeling[38]. Analysis of surface plots obtained by RSM was used for optimization and investigation of interactions between various studied factors. The mathematical model of design used is represented in a polynomial equation:

$$\begin{aligned}\hat{Y} &= \beta_0 + \beta_1 X_1 + \beta_2 X_2 + \beta_3 X_3 + \beta_{12} X_{12} + \beta_{13} X_{13} \\ &\quad + \beta_{23} X_{23} + \beta_{11} X_1^2 + \beta_{22} X_2^2 + \beta_{33} X_3^2 Y \\ &= \beta_0 + \beta_1 X_1 + \beta_2 X_2 + \beta_3 X_3 + \beta_{12} X_{12} + \beta_{13} X_{13} \\ &\quad + \beta_{23} X_{23} + \beta_{11} X_{12} + \beta_{22} X_{22} + \beta_{33} X_{32}, \end{aligned} \quad (3)$$

where, $\hat{Y}$ is theoretical response, X_i the coded variables of the system, and β_0, β_i, β_{ij}, β_{ii} are the true model coefficients. The polynomial equation obtained for each response property was analyzed using RSM for the optimization of response. Design Expert® (demo version 7.1.4, StatEase) was used for the purpose of RSM. In addition, statistical tests, such as analysis of variance (ANOVA), were performed to determine the statistical significance of each model coefficient[39]. The lack-of-fit test was also carried out for assessing the significance of selected model. If variance due to lack-of-fit is not significantly different in comparison to pure error variance, the fitted model was considered as acceptable.

In vitro drug release

In vitro release study of optimized nanoparticles formulation was performed in triplicate using dialysis membrane diffusion method[40]. Briefly, 10 mg of freeze-dried nanoparticles were dispersed in 2 mL of Milli-Q® water and transferred to a dialysis bag (Spectrapor, Molecular weight cutoff, 12 KDa) and sealed. Release studies were conducted using modified USP Type II dissolution apparatus (Electrolab, Mumbai, India). The sealed dialysis bag was placed in 50 mL of phosphate-buffered saline (pH 7.4) with Tween 80 (2%, w/v) maintained at 37 ± 2°C with continuous stirring at 50 rpm. Samples of 2 mL were withdrawn at predetermined time intervals over a period of 72 hours and replaced with same volume of fresh dissolution media. The obtained samples were centrifuged at 14,000 rpm for 10 minutes, supernatant was suitably diluted with mobile phase and analyzed by HPLC method. The obtained in vitro release data were fitted into conventional (zero order, first order, Higuchi model) and novel (reciprocal-powered time) mathematical models for evaluation of release kinetics[41]. The parameters of release kinetics regression coefficient (R^2) and time for 50% dissolution ($t_{50\%}$) were calculated for the best-fit model. Following mathematical models were used for the drug release data fitting:

$$\text{Zero order}: F = k_0 t, \tag{4}$$

$$\text{First order}: \ln(1-F) = -k_f t, \tag{5}$$

$$\text{Higuchi}: F = k_H \sqrt{t}, \tag{6}$$

$$\text{Reciprocal powered time}: \left(\frac{1}{F} - 1\right) = \frac{m}{t^b}, \tag{7}$$

where, F is the fraction of drug released up to time t. k_0, k_f, k_H, m, and b are the model parameters.

In situ rat intestinal absorption study

In situ rat intestinal absorption studies were carried out in triplicates for evaluation of the absorption properties of pure drug and optimized nanoparticle formulation[42]. Feasibility and suitability of the in situ rat intestinal absorption model for determination of absorption behavior of PCT was ensured by performing supporting studies such as solubility of PCT at tested concentration and stability of drug in buffer media for experimental duration. The nonspecific adsorption of PCT to the walls of silicone tubing was also tested by circulating the working concentration of PCT (100 µg/mL in Sorenson buffer with (1%, v/v) ethyl alcohol) for 4 hours. The percent of PCT adsorbed to silicone tubing was found to be less than 10%. The following formulations were evaluated for the absorption behavior using in situ model:

a. Pure PCT in Sorenson buffer with ethyl alcohol (1%, v/v) prepared at 100 µg/mL concentration,
b. Optimized nanoparticle formulation suspended in Sorenson buffer at concentration equivalent to 100 µg/mL of PCT.

Animals were fasted for 12–16 hours before commencement of the experiment and water was provided ad libitum. The rats were anesthetized by intraperitoneal administration of urethane (1 g/kg body weight) 1 hour prior to surgery. The abdominal region of anesthetized rat was depilated and midline abdominal incision was made. The small intestine was exposed and 10-cm length intestinal loop was prepared by inserting two silicone cannulae at the proximal end of duodenum and distal end of ileum, which were ligated tightly with the help of silk suture[43]. Extreme care was taken to ensure that no major blood vessels supplying blood to gut were blocked. The cannula at duodenum end was connected isoperistatically and other cannula at ileum was connected antiperistatically. All solutions were incubated in a water bath maintained at 37 ± 2°C. The intestinal loop was washed with 30 mL of perfusion solution (sodium chloride, 1.45×10^{-1} M; potassium chloride, 4.56×10^{-3} M; calcium chloride, 1.25×10^{-3} M; sodium dihydrogen phosphate, 5×10^{-3} M) to clear the intestinal contents. The residual perfusion solution was removed by passing air. The free ends of silicone cannulae were dipped in reservoir (10 mL of (a) or (b)) with constant stirring at ~100 rpm with the help of magnetic stirrer. The formulation was circulated at a flow rate of 0.9 mL/min and samples of 100 µL were withdrawn from the reservoir at predetermined intervals over a period of 60 minutes. The samples were centrifuged at 14,000 rpm for 10 minutes and supernatant was diluted suitably with mobile phase and analyzed by HPLC method. The experiment was performed under a closed hood in which the temperature was maintained at 37 ± 2°C with the help of heating lamps. Following termination of the experiment, the length of intestinal segment was accurately measured. The water transport was corrected, and absorption rate constant and absorption half-life were calculated from the slope obtained from the log amount remaining to be absorbed (ARA) versus time profile. The mean absorption rate constant (K_a) was calculated as K_a = slope × (–2.303) and mean absorption half-life was calculated as $t_{1/2(abs)} = 0.693/K_a$. The total flux (J), which can be expressed as the

amount of drug absorbed per unit time per unit surface area, was also determined. Student's *t*-test was applied for the statistical hypothesis testing of flux values obtained for both the treatments. The *P*-value at 5% significance level was calculated.

Results and discussion

PCT is one of the most important drugs currently available for cancer therapy due to its unique mechanisms and ability to act against various types of cancers. Considering the potential problems associated with the use of only available formulation Taxol®, it is important to develop an alternative delivery system for this drug that is devoid of toxic effects. Over the past few decades, efforts were made in developing nontoxic nanoparticulate formulations for controlled and targeted delivery of PCT. Abraxane® (Abraxis BioSciences, Los Angeles, USA) is one of those marketed formulations, in which PCT is bound to albumin and used for metastatic breast cancer treatment[20]. A novel nanopolymer-based PCT formulation Nanoxel™ (Dabur Pharma, Ghasiabad, India) contains pH-sensitive tumor targeting system that has shown improved efficacy and safety compared to Taxol®. Nanoxel™ has shown promising results in phase-I and phase-II trials for treatment of metastatic breast cancers and currently in phase-III trials[44]. Another new formulation, Nanotax® (CritiTech, Inc., Lawrence, USA) is the aqueous, stable nanocrystal suspension of PCT and targeted for ovarian and pancreatic cancers. The phase-I clinical study of Nanotax® has started in 2008 and is currently in progress[45]. In the view of current developments, the present work was initiated to develop a nanoparticulate carrier system capable of enhancing the therapeutic concentrations of PCT at target site.

Design of experimentation

Preparation of nanoparticles is a complex procedure as it involves several processing variables and design components. These variables and system components also demonstrate significant interactions among themselves that affect the quality of final product. For successful formulation development, it is extremely important to identify these critical factors and their interactions that have potential impact on quality attributes and performance characteristics of the product. The use of experimental techniques, such as DOE, is the most rational and scientific way for simultaneous identification, estimation, and analysis of influence of critical factors on the quality of final system. With the use of factorial designs, only few variables can be studied at a limited number of levels because of the fact that many experiments are required to draw a significant conclusion. Moreover, use of factorial designs only aids in identification of explanatory variables and their first-order interactions. When cost and time of each experiment is very high, use of RSM can help in analyzing first-order and second-order interactions. RCCD constitutes RSM, which can offer possibility of analyzing larger number of variables at more levels with very few experimental runs.

Nanoparticles must be manufactured with optimized processing variables and design. Even slight changes in processing and design parameters can have significant impact on the quality of final product. Unique attributes of nanoparticles like particle size and entrapment efficiency are of most importance from the biological and pharmaceutical point of view. The therapeutic efficacy of nanoparticles depends majorly on particle size as it governs drug release and tissue distribution characteristics inside the body. It has been proved that nanoparticles below 300 nm shows highest targeting to tumor through a mechanism called enhanced permeation and retention effect. It has also been demonstrated that nanoparticles smaller than 100 nm yields higher bioavailability than larger particles[46]. Another quality attribute of nanoparticles is the entrapment efficiency as it should be properly optimized to avoid the loss of drug during processing. It is of highest importance in case of drugs like PCT, where the synthesis cost is very high. In the present design, RCCD was successfully implemented for the optimization of various quality attributes of nanoparticles.

Mean particle size

The mean particle size of various batches is shown in Table 2. It can be seen from the results that the particle size ranged between 191.90 and 388.40 nm indicating the sensitivity toward the critical factors studied. The particle size has a range of twofold suggesting the fine control of the selected factors to get optimum particle size. The experiments carried out at the center points ($n = 6$) indicate the reproducibility of experiment as coefficient of variation (CV) is less than 6%. The obtained data were fitted in different designs such as

Table 3. Lack-of-fit (LOF) test for each experimental response.

Experimental response	Source of variation	Sum of squares	DF	Mean sum of squares	*F*-value	*P*-value
Mean particle size	Linear	19015.63	11	1728.69	8.99	0.0126
	2 FI[a]	15367.97	8	1921.00	9.99	0.0107
	Quadratic	4679.95	5	935.99	4.87	0.0536*
	Pure error	961.13	5	192.23		
Entrapment efficiency	Linear	280.40	11	25.49	4.38	0.0578*
	2 FI[a]	215.55	8	26.94	4.62	0.0542*
	Quadratic	65.00	5	13.00	2.23	0.1995*
	Pure error	29.13	5	5.83		

[a]Two-factor interaction. *Not significant $\alpha < 0.05$ (no lack-of-fit).

linear, two-factor interaction, and quadratic models to select the best model that describes the relationship between critical factors and response. The results are shown in Table 3. The quadratic model was selected as best-fit model as the *P*-value is not significant at 5% level. The statistical analysis of results (RSM) using quadratic model generated the following second-order polynomial equation for mean particle size:

$$\begin{aligned}\text{Mean particle size (nm)} &= 248.563 + (-3.084)X_1 \\ &+ (26.767)X_2 + (-26.207)X_3 + (20.363)X_{12} \\ &+ (-6.138)X_{13} + (1.913)X_{23} + (11.745)X_1^2 \\ &+ (25.492)X_2^2 + (6.146)X_3^2.\end{aligned} \quad (8)$$

The regression coefficient (R^2) of this equation was found to be 0.8563 indicating the good correlation between response and selected factors. The residuals were distributed randomly around zero and, moreover, there was no effect of experimental sequence on the trend of residuals. The obtained model coefficients were subjected to ANOVA for assessing the statistical significance. The results of ANOVA presented in Table 4 indicate the significance of model coefficients at 5% level. The obtained polynomial equation was used for RSM and three-dimensional surface plots were generated (Figure 1).

Out of the three factors studied, the amount of polymer and duration of ultrasonication were found to have considerable effect on the mean particle size. It can be seen from the three-dimensional surface plots (Figure 1) that an increase in the polymer concentration leads to the remarkable increase in the mean particle size. This may be due to the fact that excess polymer leads to increase in viscosity of polymer solution. High viscosity of polymeric solution slows down the rapid dispersion of organic phase into aqueous phase resulting in the formation of bigger aggregates. Increase in the duration of ultrasonication resulted in decreased mean particle size. It can be due to the fact that the longer duration of ultrasonication results in increased energy input to the system, thus preventing the agglomeration of particles. It is clear from Figure 1a that the optimum particle size can be achieved by taking lesser polymer coupled with higher ultrasonication times. Even though the amount of miglyol did not show statistically significant impact on the mean particle size, it can be seen from Figure 1b that an increase in miglyol proportion leads to decrease in the mean particle size. This observation can be supported by the theory of stable emulsification as the miglyol fraction aids in reducing surface tension and facilitates low mean particle size. Moreover, the first-order interaction of miglyol with polymer was found to be statistically significant. As indicated in Figure 1c, optimum particle size can be achieved with suitable polymer content and little miglyol. Higher miglyol content coupled with very less or very high polymer amount leads to dramatic increase in the mean particle size.

Entrapment efficiency

The entrapment efficiencies of individual batches of prepared nanoparticulate formulations are presented in Table 2. The entrapment efficiency ranged between

Table 4. Analysis of variance (ANOVA) test for each experimental response.

	Mean particle size				Entrapment efficiency			
Source	Sum of squares	DF	*F*-value	*P*-value	Sum of squares	DF	*F*-value	*P*-value
Model	33613.79	9	6.62	0.0034*	638.93	9	7.54	0.0020*
X_1	130.84	1	0.23	0.6405	0.61	1	0.065	0.8042
X_2	9775.99	1	17.33	0.0019*	295.34	1	31.37	0.0002*
X_3	9371.28	1	16.61	0.0022*	127.58	1	13.55	0.0042*
X_{12}	3317.05	1	5.88	0.0358*	0.25	1	0.026	0.8750
X_{13}	301.35	1	0.53	0.4816	26.06	1	2.77	0.1271
X_{23}	29.26	1	0.052	0.8244	38.54	1	4.09	0.0706
X_1^2	1976.77	1	3.50	0.0907	21.96	1	2.33	0.1577
X_2^2	9337.79	1	16.55	0.0023*	123.03	1	13.07	0.0047*
X_3^2	543.37	1	0.96	0.3495	5.56	1	0.59	0.4600
Residual	5641.08	10			94.13	10		
Lack-of-fit	4679.75	5	4.87	0.0536*	65.00	5	2.23	0.1995*
Pure error	961.13	5			29.13	5		
Total	39524.87	19			733.06	19		

*Significant at $\alpha < 0.05$. **Not significant at $\alpha < 0.05$ (no lack-of-fit).

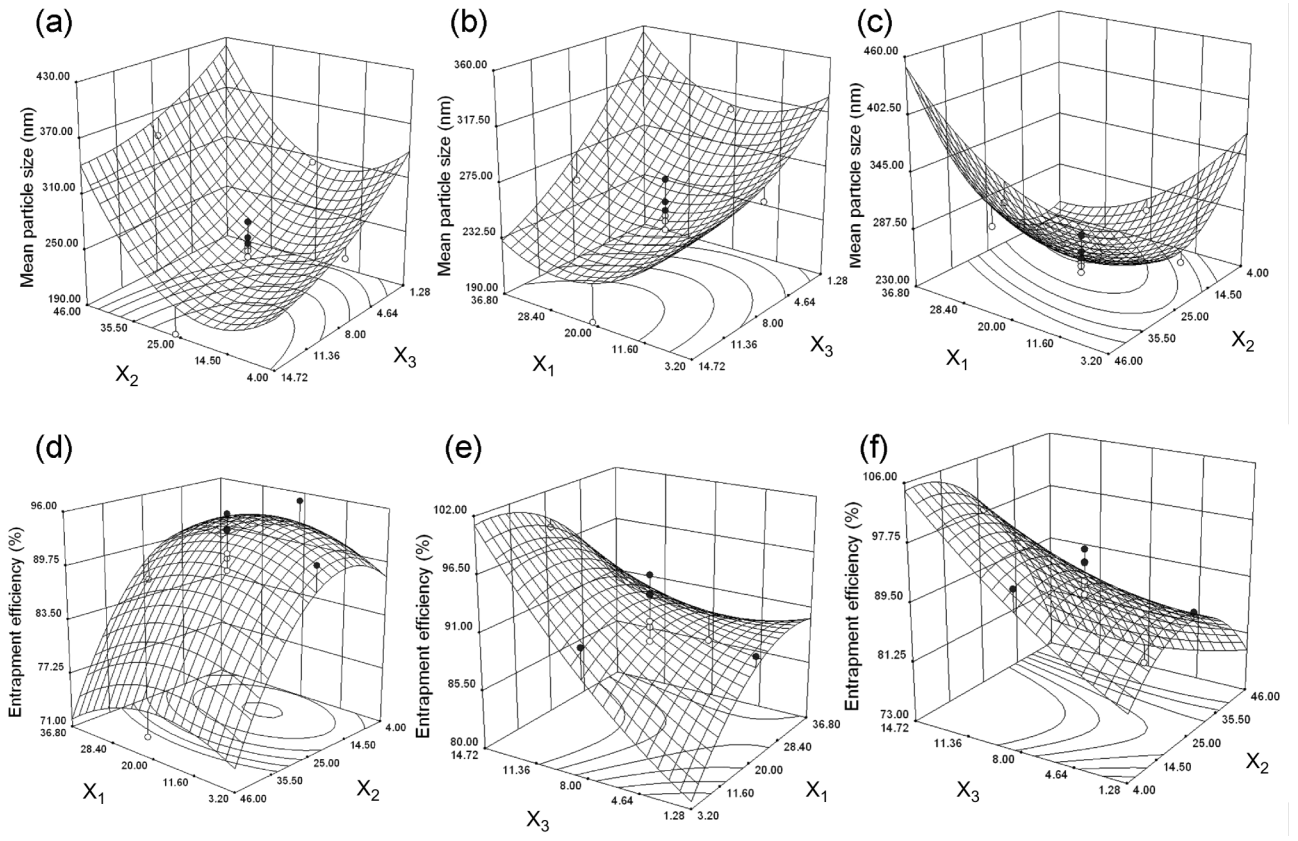

Figure 1. Response surface plots of mean particle size and entrapment efficiency versus two factors (third factor was held at optimum level): X_1 = amount of miglyol, X_2 = amount of polymer, X_3 = duration of ultrasonication at 15 W.

73.37% and 98.41%, which indicate that the response was sensitive toward the studied factors. The experiments performed at the center points confirmed that the experimental method was highly reproducible (CV < 3%). Data presented in Table 3 indicate that the selected quadratic model well-describes the relationship between the entrapment efficiency and critical factors with *P*-value not being significant at 5% level. The selected quadratic model was used to generate the following second-order polynomial equation for the entrapment efficiency:

$$\begin{aligned}&\text{Entrapment efficiency}\,(\%) = 92.3369 + (-0.2124)X_1 \\ &+(-4.6526)X_2 + (3.0571)X_3 + (-0.1761)X_{12} \\ &+(-1.8064)X_{13} + (2.1952)X_{23} + (-1.2368)X_{12} \\ &+(-2.9262)X_2^2 + (0.6228)X_3^2.\end{aligned} \tag{9}$$

The regression value of the above equation was found to be 0.8716 indicating suitability of the selected model. The analysis of residuals indicated that the residuals were normally distributed around zero. Moreover, the experimental order did not impact the residual trend. The results of ANOVA are listed in Table 4, which indicate the statistical significance of model coefficients. Equation (9) was also used to generate three-dimensional response surface plots by keeping one factor at optimum level (Figure 1).

Amount of polymer and duration of ultrasonication were found to have significant effect on the entrapment efficiency. Figure 1d indicates an exponential relationship between entrapment efficiency and the amount of polymer. Initial increase in the amount of polymer resulted in proportionate increase in the entrapment efficacy. However, if the amount of polymer is increased beyond an optimum value, the entrapment efficiency was found to be decreased. On the contrary, an increase in the duration of ultrasonication resulted in a proportionate increase in the entrapment efficiency indicating a linear relationship (Figure 1e). This may be because of the fact that the high energy provided by ultrasonication helped in preventing drug leaching out from the particles thus increasing the entrapment efficiency. Even though amount of miglyol did not show statistical significance, it can be seen from Figure 1e that increase in miglyol till optimum value increased the entrapment efficiency. This increase can be due to the fact that

Table 5. Optimized formulation conditions offered by software.

				Predicted values		Experimental values[a]	
Batch no.	X_1 (μL)	X_2 (mg)	X_3 (minutes)	Mean particle size (nm)	Entrapment efficiency (%)	Mean particle size (nm)[b]	Entrapment efficiency (%)[b]
1	33.80	10.38	14.72	192.65	98.41	231.68 ± 10.41	95.18 ± 1.54
2	34.00	9.25	14.72	192.89	98.43	252.32 ± 14.04	93.71 ± 2.16

[a]Each batch was prepared three times. [b]Each value is expressed as mean ± SD.

miglyol acts as a core for drug to entrap drug into the polymeric matrix forming nanoparticles. However, beyond optimum value, due to the lack of amount of polymer and duration of ultrasonication there is no further enhancement in the entrapment efficiency.

The suitable conditions of three critical factors for optimum particle size (<250 nm) and entrapment efficiency (>90%) were obtained by software based on the principles of numerical optimization. The conditions offered by the software are shown in Table 5. Desirability factor (D, $0 < D < 1$) was determined for each formulation in Table 5. Desirability factor 0 indicates the property level that is not acceptable for product usage. Desirability factor 1 represents property level at which small changes may not improve the quality of the final product. The calculated desirability factor was greater than 0.976 for both formulations indicating higher 'desirability' of corresponding response properties. Each formulation was prepared three times, and the mean particle size and entrapment efficiency were estimated. The predicted results along with observed values are shown in Table 5. Even though the error value obtained for entrapment efficiency is very less, distinct deviations were observed for mean particle size. This may be due to the presence of some minor contributing factors, which were not considered during the experiment. Hence, the optimum formulation with mean particle size 231.68 ± 10.41 nm and entrapment efficiency 95.18 ± 1.54% can be achieved with 33.80 μL of miglyol, 10.38 mg of polymer, and 14.72 minutes of ultrasonication duration at 15 W. The drug content and polydispersity index of the optimized batch is found to be 4.88 ± 0.265% and 0.232 ± 0.018, respectively.

In vitro drug release

The in vitro drug release profile of optimized nanoparticulate formulation is presented in Figure 2. The nanoparticulate formulation provided a biphasic drug release pattern, which was characterized by an initial burst release of PCT followed by a slow and continuous drug release for 72 hours. The initial burst release may be attributed to the dissolution of poorly entrapped drug from the surface of nanoparticles. The later phase providing a slow release may have been resulted from slow dissolution and diffusion of the entrapped drug

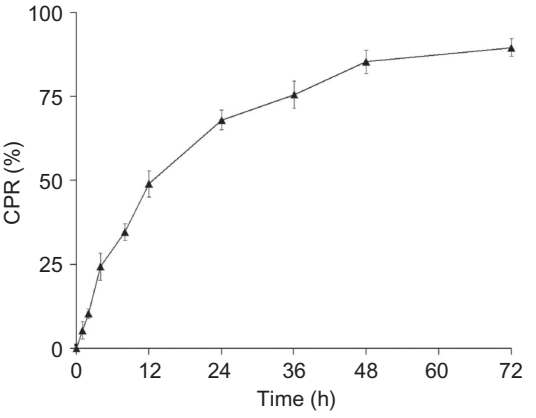

Figure 2. In vitro drug release study of optimized nanoparticle formulation (CPR, % cumulative paclitaxel released) (mean ± SD, $n = 3$).

from the polymeric matrix of nanoparticles. The drug release kinetics was studied by fitting the data into various mathematical models. The regression analysis indicated that drug release from nanoparticles can be well explained by reciprocal-powered time model (r^2 = 0.9957) compared with zero-order kinetics (r^2 = 0.8208), first-order kinetics (r^2 = 0.9648), and Higuchi kinetics (r^2 = 0.9622). Previously, Barzegar-Jalali et al. have reported that the reciprocal-powered time model is the most suitable model to study the drug release kinetics from nanoparticulate formulations[41]. The $t_{50\%}$ value obtained from the reciprocal-powered time model was found to be 12.10 hours.

In situ rat intestinal absorption study

The semi-logarithmic graph between ARA and time for both the formulations is shown in Figure 3. The regression analysis for both the treatments ($R^2 > 0.95$) indicated an exponential disappearance of the drug from the intestine. Figure 3 indicates that the nanoparticulate formulation is rapidly absorbed compared with the pure drug. It is evident from the literature that because of their submicron size, nanoparticles absorbs rapidly and breaches through various biological barriers. The mean absorption rate constant (K_a) for the optimized nanoparticulate formulation (0.311 ± 0.018 hour^{-1}) was found to be 1.5-fold higher than that

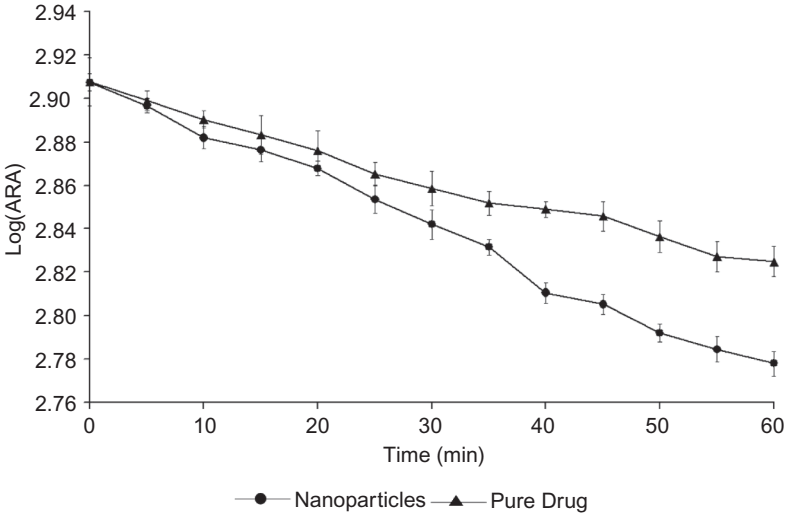

Figure 3. In situ rat intestinal absorption study of pure drug and optimized nanoparticles formulation (ARA, amount remaining to be absorbed) (mean ± SD, $n = 3$).

observed for the pure drug (0.190 ± 0.009 hour^{-1}). The high mean absorption rate constant indicated a rapid absorption of the drug from the prepared nanoparticles. The mean absorption half-life ($t_{1/2}$) for optimized nanoparticle (2.23 ± 0.130 hours) was found to be significantly lesser than that of the pure drug (3.65 ± 0.167 hours). Similarly, the total flux (J) observed for the optimized nanoparticulate formulation (20.47 ± 2.933 μg/h/cm^2) was higher than that of the pure drug (13.78 ± 0.700 μg/h/cm^2). Student's t-test revealed a statistically significant difference between flux values obtained for both treatments ($P = 0.0184$). Overall, there was 48.57% increase in the extent of PCT absorption from the nanoparticulate formulation compared with the pure drug. Thus, the optimized nanoparticulate formulation may enhance the drug bioavailability resulting in higher plasma levels of PCT compared with the pure drug.

Conclusion

In the present study, nanoparticles of PCT were prepared aiming to develop a safe and effective formulation that is devoid of Cremophor EL. Simple emulsion solvent evaporation technique was found to be effective and reproducible in the preparation of PLGA nanoparticles containing PCT. Various processing critical variables in the preparation method were identified and optimized by a scientifically efficient RCCD design. The optimized formulation provided a uniform small particle size with high entrapment efficiencies. In vitro release study confirmed that the entrapped drug is released over 72 hours in a corolled manner. Moreover, the in situ rat intestinal absorption study demonstrated a rapid absorption of the drug with increased extent of absorption from nanoparticles in comparison with the pure drug. Based on these findings, it can be concluded that the proposed nanoparticle formulation may demonstrate enhanced oral bioavailability, increased plasma levels, and faster onset of action in clinical studies.

Acknowledgments

The authors are thankful to Dr. Reddy's Laboratories, India, and Purac, USA, for their generous gift samples of PCT and PLGA, respectively. The authors are also grateful to Panacea Biotec, India, for extending their facility for PCS analysis.

Declaration of interest

The authors report no conflicts of interest. The authors alone are responsible for the content and writing of this paper.

References

1. Inbar M, Merimsky O, Chaitchik S. (1997). Taxanes: A breakthrough in cancer chemotherapy. Harefuah, 133(1–2):31–6.
2. Schiff PB, Fant J, Horwitz SB. (1979). Promotion of microtubule assembly in vitro by taxol. Nature, 277:665–7.
3. Schiff PB, Horwitz SB. (1981). Taxol stabilizes microtubules in mouse fibroblast cells. Biochemistry, 20:3247–52.
4. Haldar S, Chintapalli J, Croce CM. (1996). Taxol induces Bcl-2 phosphorylation and death of prostate cancer cells. Cancer Res, 56:1253–5.

5. Spencer CM, Faulds D. (1994). Paclitaxel—a review of its pharmacodynamic and pharmacokinetic properties and therapeutic potential in the treatment of cancer. Drugs, 48(5):794–847.
6. Ishitobi M, Shin E, Kikkawa N. (2001). Metastatic breast cancer with resistance to both anthracycline and docetaxel successfully treated with weekly paclitaxel. Int J Clin Oncol, 6(1):55–8.
7. Thigpen JT. (2000). Chemotherapy for advanced ovarian cancer: Overview of randomized trials. Semin Oncol, 27(3):11–6.
8. Chang AY, Rubins J, Asbury R, Boros L, Hui LF. (2001). Weekly paclitaxel in advanced non-small cell lung cancer. Semin Oncol, 28(4):10–3.
9. Li KW, Dang W, Tyler BM, Troiano G, Thian T, Brem H, et al. (2003). Polilactofate microspheres for paclitaxel delivery to central nervous system malignancies. Clin Anticancer Res, 15(9):3441–7.
10. Fellner S, Bauer B, Miller DS, Schaffrik M, Fankhanel M, Sprub T, et al. (2002). Transport of paclitaxel (Taxol) across the blood-brain barrier in vitro and in vivo. J Clin Invest, 10(9):1309–17.
11. Rowinsky EK, Cazenave LA, Donehower RC. (1990). Taxol: A novel investigational antimicrotubule agent. J Natl Cancer Inst, 82:1247–59.
12. Nakajima M, Fujiki Y, Kyo S, Kanaya T, Nakamura M, Maida Y, et al. (2005). Pharmacokinetics of paclitaxel in ovarian cancer patients and genetic polymorphisms of CYP2C8, CYP3A4, and MDR1. J Clin Pharmcol, 45:674–82.
13. Gallo JM, Li S, Guo P, Redd K, Ma J. (2003). The effect of P-glycoprotein on paclitaxel brain and brain tumor distribution in mice. Cancer Res, 63:5114–7.
14. Kemper EM, van Zandbergen AE, Cleypool C, Mos HA, Boogerd W, Beijnen JH, et al. (2003). Increased penetration of paclitaxel into the brain by inhibition of P-glycoprotein. Clin Cancer Res, 9:2849–55.
15. Weiss R, Donehower RC, Wiernik PH. (1990). Hypersensitivity reactions from taxol. J Clin Oncol, 8:1263–8.
16. Friedland D, Gorman G, Treat J. (1993). Hypersensitivity reactions from taxol and etoposide. J Natl Cancer Inst, 85(24):2036.
17. Gregory R, DeLisa AF. (1993). Paclitaxel: A new antineoplastic agent for refractory ovarian cancer. Clin Pharm, 42:401–15.
18. Fjallskog ML, Frii L, Bergh J. (1993). Is Cremophor EL, solvent for paclitaxel, cytotoxic? Lancet, 342(8875):873.
19. Singla AK, Garg A, Aggarwal D. (2002). Paclitaxel and its formulations. Int J Pharm, 235:179–92.
20. Ibrahim NK, Samuels B, Page R, Doval D, Patel KM, Rao SC, et al. (2005). Multicenter phase II trial of ABI-007, an albumin-bound paclitaxel, in women with metastatic breast cancer. J Clin Oncol, 23(25):6019–26.
21. Sharma A, Straubinger RM. (1994). Novel Taxol formulations: Preparation and characterization of Taxol-containing liposomes. Pharm Res, 11:889–95.
22. Gupte A, Ciftci K. (2004). Formulation and characterization of paclitaxel, 5-FU and paclitaxel + 5-FU microspheres. Int J Pharm, 276(1–2):93–106.
23. Liggins RT, Cruz T, Min W, Liang L, Hunter WL, Burt HM. (2004). Intra-articular treatment of arthritis with microsphere formulations of paclitaxel: Biocompatibility and efficacy determinations in rabbits. Inflamm Res, 53(8):363–72.
24. Lundberg BB. (1997). A submicron lipid emulsion coated with amphipathic polyethylene glycol for parenteral administration of paclitaxel (Taxol). J Pharm Pharmacol, 49(1):16–21.
25. Tarr BD, Sambandan TG, Yalkowsky SH. (1987). A new parenteral emulsion for the administration of Taxol. Pharm Res, 4(2):162–5.
26. Yegin BA, Benoît JP, Lamprecht A. (2006). Paclitaxel-loaded lipid nanoparticles prepared by solvent injection or ultrasound emulsification. Drug Dev Ind Pharm, 32(9):1089–94.
27. Si-Shen F, Li M, Win KY, Guofeng H. (2004). Nanoparticles of biodegradable polymers for clinical administration of paclitaxel. Curr Med Chem, 11(4):413–24.
28. Yang S, Gursoy RN, Lambert G, Benita S. (2004). Enhanced oral absorption of paclitaxel in a novel self-microemulsifying drug delivery system with or without concomitant use of p-glycoprotein inhibitors. Pharm Res, 21(2):261–70.
29. Wang J, Mongayt D, Torchilin VP. (2005). Polymeric micelles for delivery of poorly soluble drugs: Preparation and anticancer activity in vitro of paclitaxel incorporated into mixed micelles based on poly(ethylene glycol)-lipid conjugate and positively charged lipids. J Drug Target, 13(1):73–80.
30. Couvreur P, Kante B, Lenaerts V, Scailteur V, Ronald M, Speiser P. (1980). Tissue distribution of antitumor drugs associated with polyalkylcyanoacrylate nanoparticles. J Pharm Sci, 69(2):199–202.
31. Peppas LB, Blanchette JO. (2004). Nanoparticles and targeted systems for cancer therapy. Adv Drug Deliv Rev, 56:1649–59.
32. Bennis S, Chapey C, Couvreur P, Robert J. (1994). Enhanced cytotoxicity of doxorubicin encapsulated in polyisohexylcyanoacryate nanospheres against multidrug-resistant cells in culture. Eur J Cancer, 30A(1):89–93.
33. Guerrero DQ, Allemann E, Fessi H, Doelker E. (1998). Preparation techniques and mechanisms of formation of biodegradable nanoparticles from preformed polymers. Drug Dev Ind Pharm, 24(12):1113–28.
34. Agnihotri SA, Aminabhavi TM. (2007). Chitosan nanoparticles for prolonged delivery of timolol maleate. Drug Dev Ind Pharm, 33(11):1254–62.
35. Graves RA, Poole D, Moiseyev R, Bostanian LA, Mandal TK. (2008). Encapsulation of indomethacin using coaxial ultrasonic atomization followed by solvent evaporation. Drug Dev Ind Pharm, 34(4):419–26.
36. Attivi D, Wehrle P, Ubrich N, Damge C, Hoffman M, Maincent P. (2005). Formulation of insulin-loaded polymeric nanoparticles using response surface methodology. Drug Dev Ind Pharm, 31(2):179–89.
37. Shi K, Cui F. (2009). Optimized formulation of high-pay load PLGA nanoparticles containing insulin–lauryl sulfate complex. Drug Dev Ind Pharm, 35(2):177–84.
38. Akhnazarova S, Kafaro V. (1982). Experiment optimization in chemistry and chemical engineering. Moscow: Mir House Publications.
39. Bolton S. (1997). Pharmaceutical statistics: Practical and clinical applications. New York: Marcel Dekker.
40. Levy MY, Benita S. (1990). Drug release from submicronized o/w emulsion: A new in vitro kinetic evaluation model. Int J Pharm, 66(1–3):29–37.
41. Barzegar-Jalali M, Adibkia K, Valizadeh H, Shadbad MRS, Nokhodchi A, Omidi Y, et al. (2008). Kinetic analysis of drug release from nanoparticles. J Pharm Pharm Sci, 11(1):167–77.
42. Doluisio JT, Bilups NF, Tukker JJ, Crommelin DJA. (1969). Drug absorption I: An in-situ rat gut technique yielding realistic absorption rates. J Pharm Sci, 58:1197–8.
43. Schurgers N, Bijdendijk J, Tukker JJ, Crommelin DJA. (1986). Comparison of four experimental techniques for studying drug absorption kinetics in the anesthetized rat in situ. J Pharm Sci, 75(2):117–9.
44. Singh AT, Jaggi M, Khattar D, Awasthi A, Mishra SK, Tyagi S, et al. (2008). A novel nanopolymer based tumor targeted delivery system for paclitaxel. J Clin Oncol, 26(15S):11095.
45. Niu F, Roby KF, Rajewski RA, Decedue C, Subramaniam B. (2006). Polymeric drug delivery II: Polymeric matrices and drug particle engineering. Washington, DC: ACS Publications.
46. Jani P, Halbert GW, Langridge J, Florence AT. (1990). Nanoparticle uptake by the rat gastrointestinal mucosa: Quantitation and particle size dependency. J Pharm Pharmacol, 42(12):821–6.